BEAM ENERGY MEASUREMENTS IN THE FLASH INJECTOR USING SYNCHROTRON RADIATION AND BUNCH ARRIVAL MONITORS

Ch. Gerth, M. K. Bock, M. Hoffmann, F. Ludwig, H. Schlarb and C. Schmidt
Deutsches Elektronen-Synchrotron DESY, D-22603 Hamburg, Germany

Abstract

The high beam energy stability required for stable operation of linac-driven free-electron lasers demands for precise cavity RF field regulation. This is in particular true for the accelerator modules at low beam energies which are used to induce an energy correlation on the electron beam for longitudinal bunch compression in magnetic chicanes. For the validation and optimization of the cavity field regulation, several beam-based techniques have recently been developed which can be used to monitor the beam energy with high precision or as fast feedbacks for the RF regulation. In this paper, we report on bunch-resolved energy measurements recorded independently with a synchrotron radiation monitor and two bunch arrival monitors in the injector at FLASH. Good agreement between the monitors was found and the measurement data are compared with the results from RF field detection.

INTRODUCTION

Ultra-short electron bunches with high peak currents are required to drive a high-gain free-electron laser (FEL). These ultra-short bunches are commonly produced by inducing a longitudinal energy correlation on the bunch which leads to longitudinal bunch compression in magnetic chicanes. Small fluctuations in the RF accelerating fields that induce the energy chirp for bunch compression lead to variations in the energy chirp rate and may cause unacceptable peak current and bunch arrival time jitters. For instance in the injector at FLASH, RF amplitude and phase stabilities of about 10^{-4} and 0.01° are required to keep peak current variations below the percent level.

A schematic of the FLASH injector is shown in Fig. 1. The normal-conducting 1.3 GHz RF photo-cathode gun is followed by two super-conducting (sc) accelerating modules which operate at $f_1 = 1.3$ GHz (ACC1) and $f_3 = 3 \times F_1 = 3.9$ GHz (ACC39). The module ACC39 has been installed in early 2010 and is used for linearisation of the longitudinal phase space for bunch compression. The injector can be operated with 800 μs long flattop pulses with 1 MHz bunch spacing and 10 Hz bunch train repetition rate with a typical beam energy of 150 MeV. The sc modules comprise 9-cell niobium cavities with a very high quality factor, i.e. very narrow bandwidths and long response times. The RF controller in the digital control loop of the low-level RF (LLRF) system has an adjustable feedback gain g for the RF field regulation.

The accelerating modules are followed by a bunch compressor (BC) consisting of a 4 dipole chicane. Any deviation $\Delta E/E$ from the nominal beam energy transforms into a horizontal beam displacement Δx in the dispersive section of the BC and a beam arrival time difference Δt after the BC given by (first order transport theory, $\beta \simeq 1$):

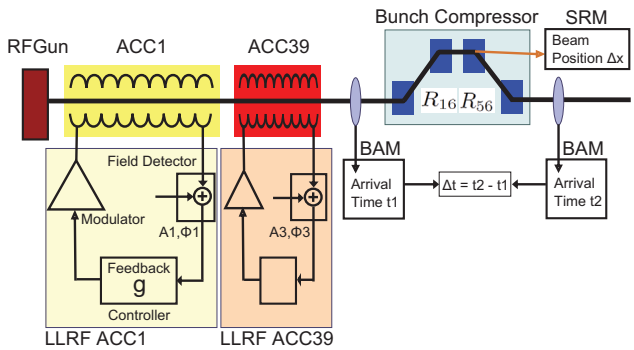

Figure 1: Schematic of FLASH injector.

$$\Delta x = R_{16} \cdot \frac{\Delta E}{E} \quad \text{and} \quad \Delta t = R_{56}/c \cdot \frac{\Delta E}{E}, \qquad (1)$$

where $R_{16} \approx 300 - 400$ mm and $R_{56} \approx 140 - 230$ mm are the horizontal and longitudinal dispersions of the BC. Beam energy deviations can be determined by recording variations of either the beam position Δx with a synchrotron radiation monitor (SRM) located behind the 3^{rd} dipole of the BC or flight time Δt with two bunch arrival time monitors (BAMs) up- and downstream of the BC.

MONITOR SETUPS

The synchrotron radiation emitted in the third dipole of the BC can be recorded by the SRM which comprises an intensified CCD camera [1] and a multi-anode photomultiplier tube (PMT) [2]. By utilizing a beam splitter, both the CCD camera and PMT can be used simultaneously.

A commercial photo lens ($f = 300$ mm) and teleconverter (x3.0) are used to image the synchrotron radiation onto two adjacent anodes of the PMT. The fast PMT signals are sampled by analog-to-digital converters (ADC) with bunch-synchronous read-out. The centre-of-gravity beam position can be expressed by the normalized difference signal s of both anodes:

$$s = \frac{I_1 - I_2}{I_1 + I_2}, \qquad (2)$$

where I_1 and I_2 are the signal intensities of each anode. By normalizing the difference signal s, an influence of a bunch charge jitter on the difference signal is eliminated.

ISBN 978-3-95450-117-5

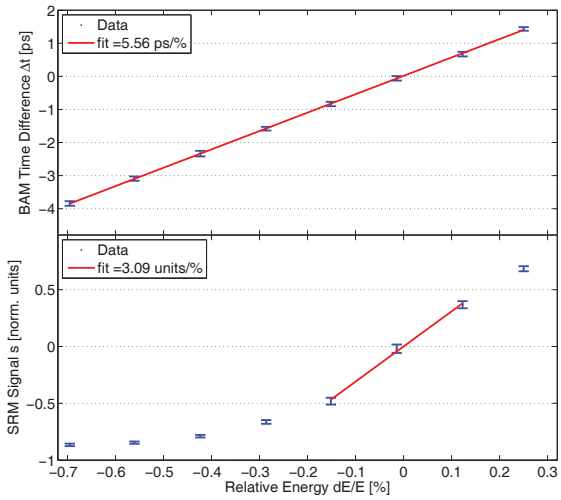

Figure 2: Energy calibration of the BAMs (top) and SRM (bottom) at on-crest operation.

The BAM [3] measures the arrival time of the bunches relative to laser pulses which are distributed from a master laser-oscillator [4] via actively length-stabilised fibre links with femtosecond timing stability. The electron bunches induce high-frequency (bw $>$ 10 GHz) voltage signals in the BAM pick-up, which are sent to an electro-optical modulator (EOM) in the optical BAM front-end which is located in close proximity to the BAM pick-up. The fast transient voltage signals modulate the amplitude of a laser pulse in the EOM depending on the arrival time of the electron bunches. The pulse intensities of the modulated laser pulses are then transformed by a photo-detector into current pulses which are sampled by a fast ADC with 108 MHz sampling rate. Each measured laser pulse intensity is normalised to the previous one in order to reduce distortions due to changes of the bias voltage, EOM temperature or polarization in the link fibre. By recording the bunch arrival time difference $\Delta t = t_2 - t_1$ between the BAMs down- and upstream of the BC, variations in the flight time through the BC can be measured.

MONITOR PERFORMANCE

A relative change of the magnetic field in the BC dipoles corresponds to a relative change in beam energy $\Delta E/E$. A relative energy calibration can be performed by varying the current of the dipoles and recording the SRM signal s and flight time difference Δt with the two BAMs. The result of a calibration measurement for which ACC1 and ACC39 were operated on-crest is shown in Fig. 2. The calibration constants for the BAMs and SRM have been determined by a linear fit and amount to 5.56 ps/% and 3.1 1/%, respectively. The range for which the SRM shows a linear dependency is extremely limited ($\Delta E/E = \pm 0.1\%$) due to the narrow horizontal beam size at on-crest operation.

An upper limit for the energy resolution can be determined experimentally by recording simultaneously the relative energy jitter of two adjacent bunches in a bunch train. Figure 3 shows the correlation of the energy jitter measured with the BAMs and SRM for 500 subsequent bunch trains. Assuming that the resolution is identical for each bunch, the single-bunch energy resolution for the BAMs and SRM reduce by a factor $1/\sqrt{2}$ and amount to $4.4 \pm 0.1\ 10^{-5}$ and $4.2 \pm 0.2\ 10^{-5}$, respectively.

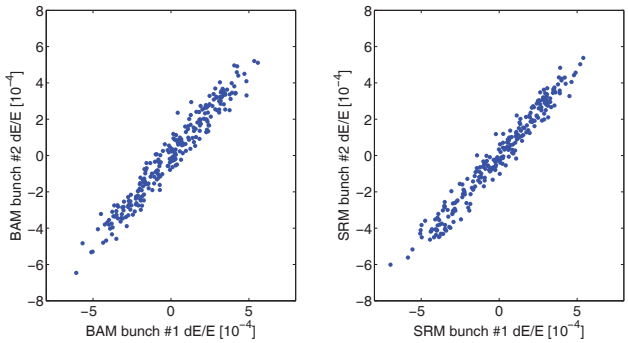

Figure 3: Correlation plot for 500 bunches recorded simultaneously with the SR-PMT and SR-camera.

The same measurements were repeated under SASE operation conditions and the calibration plot for both monitors is shown in Fig. 4. While the calibration constant of the BAMs is independent of the operation mode, the calibration constant of the SRM has decreased by a factor of about 5 to 0.61 1/%. This behaviour is also reflected in the correlation measurement. Whereas the resolution of the BAMs decreased only slightly compared to on-crest operation, the resolution of the SRM decreased drastically by a factor of about 4 to $1.6 \pm 0.2\ 10^{-4}$. At SASE operation, the bunches have a larger correlated energy distribution which

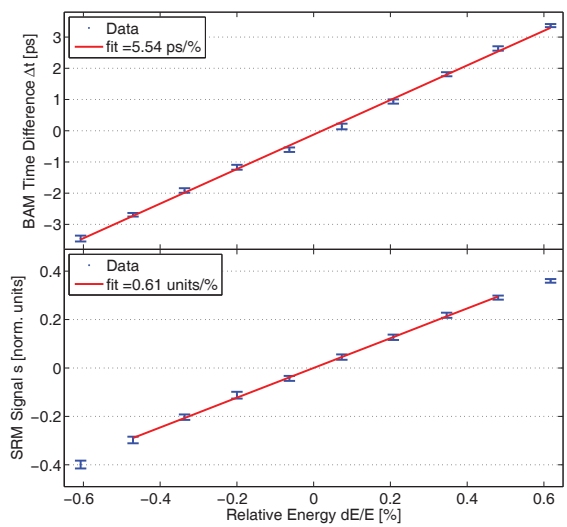

Figure 4: Energy calibration of the BAMs (top) and SRM (bottom) at SASE operation.

ISBN 978-3-95450-117-5

leads to a wider but flatter beam image on the anodes of the SRM PMTs.

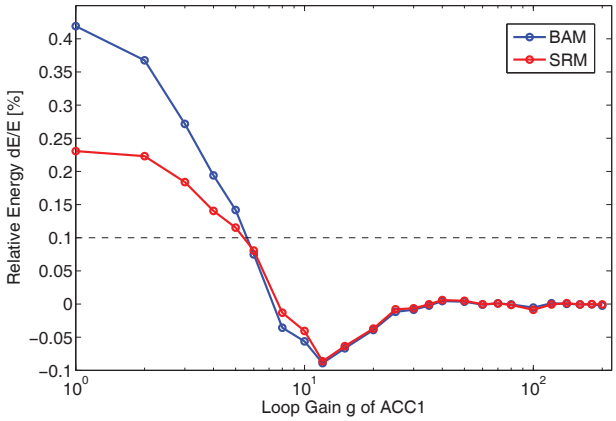

Figure 5: Relative mean energy versus ACC1 loop gain g measured with the BAMs and SRM at on-crest operation.

MEASUREMENTS

To study the performance of the LLRF system with the BAMs and SRM, the feedback controller of ACC1 (see Fig. 1) was operated as a simple proportional controller for which the loop gain g was varied between 0 and 200. The relative variation of the mean energy, measured with the BAMs and SRM at on-crest operation, is depicted in Fig. 5. For each gain setting g, 500 subsequent bunch trains with 30 bunches were recorded. The curve shows the typical behaviour of a proportional controller: The residual control loop error reduces for $g \approx 0 - 9$, then an overshoot occurs for $g \approx 9 - 40$ until a plateau is reached for which the control loop error is minimized. The relative energies measured with the SRM for $g < 5$ are too low due to the limited dynamic range ($\Delta E/E = \pm 0.1\%$, cf. Fig. 2).

The corresponding amplitude and phase jitter recorded by the RF field detection of the LLRF system during the gain scan is shown in Fig. 6. The amplitude and phase jitter reduces for increasing loop gain until a minimum is reached around $g \approx 80$. For larger loop gain values the jitter starts to increase again. The amplitude and phase jitter of ACC39, which was operated at fixed loop gain, remains constant during the ACC1 gain scan and is shown for reference. The mean energy for the bunch centre is given by ($\beta \simeq 1$):

$$\bar{E} = A_1 \cos(\phi_1) + A_3 \cos(\phi_3) + E_{gun} \text{ (in [eV])}, \quad (3)$$

where A_n and ϕ_n are the amplitudes and phases of the accelerating voltages of ACC1 ($n = 1$) and ACC39 ($n = 3$), and E_{gun} the beam energy from the RF gun. Applying Eq. 3 and Gaussian error propagation, the relative energy jitter was determined for each gain setting by calculating first the standard deviation of the 500 shots for each bunch and then the mean value of these standard deviations for the 30 bunches. The result is compared to values measured

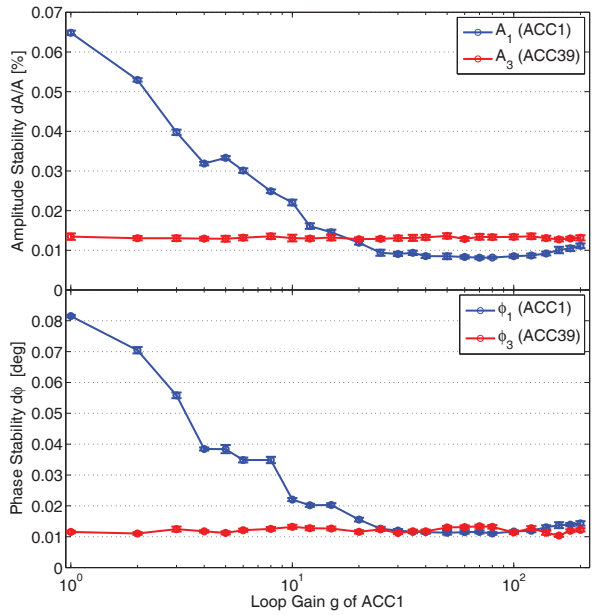

Figure 6: Relative amplitude and phase jitter as detected by the LLRF system jitter during ACC1 loop gain scan.

with the BAMs and SRM in Fig. 7. The energy jitter exhibits a weak dependency on the loop gain in the range $g \approx 40 - 140$ and has its minimum at about $g \approx 80$ for all 3 devices with values of $7.6 \pm 0.3\ 10^{-5}$ and $7.9 \pm 0.4\ 10^{-5}$ measured with the BAMs and SRM, respectively. The resolution of the LLRF system, estimated from the correlation of the energies of adjacent bunches (as described above for the BAM and SRM), amounts to $9.0\ 10^{-5}$, and the recorded energy jitter in Fig. 7 seems to be resolution limited.

The same measurements were repeated under SASE operation conditions. The variation of the mean energy (Fig. 8) shows a similar overall behaviour as the corre-

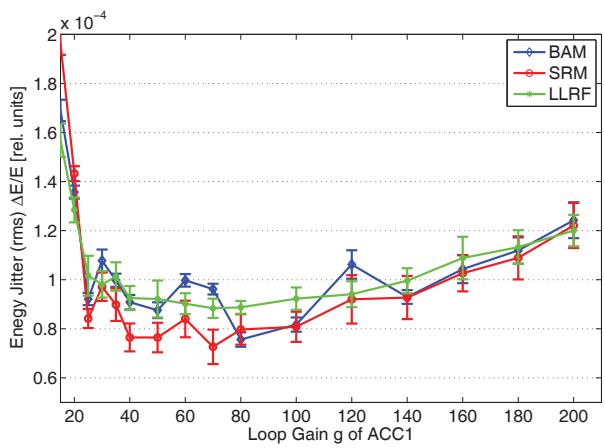

Figure 7: Relative energy jitter versus ACC1 loop gain g obtained with the BAMs, SRM and LLRF system at on-crest operation.

ISBN 978-3-95450-117-5

sponding one for on-crest operation (Fig. 5). The results of the SRM measurements are in better agreement with the BAM data for $g < 5$ due to the larger dynamic range of the SRM at SASE operation. However, the SRM data start to deviate for $\Delta E/E \geq 0.2\%$ and the difference is 0.05% at $\Delta E/E = 0.4\%$.

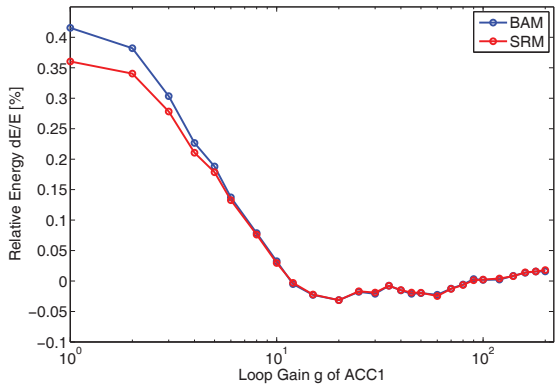

Figure 8: Relative mean energy versus ACC1 loop gain g measured with the BAMs and SRM at SASE operation.

Figure 9 presents the relative energy jitter at SASE operation measured with the BAMs and SRM and determined from the in-loop amplitudes and phases of the LLRF controller. All 3 devices show the same overall behaviour, and the energy jitter is almost constant within the error bars in the range $g \approx 35 - 100$ for each device. However, the minimum energy jitter measured with the SRM amounts to $1.9\ 10^{-4}$ which is clearly resolution limited as the resolution was determined to be $1.6 \pm 0.2\ 10^{-4}$ at SASE operation conditions. The smallest values for the energy jitter of just below $1.0\ 10^{-4}$ were determined from the data recorded by the RF field detection of the LLRF system.

CONCLUSIONS

The performance of two BAMs and a SRM for relative beam energy measurements has been determined at on-crest and SASE operation. Both devices were found to have a similar resolution at on-crest operation of about $\Delta E/E \simeq 4 - 5 \cdot 10^{-5}$. However, the SRM has a very limited dynamic range of about $\Delta E/E \approx \pm 0.1\%$ due to the narrow horizontal beam profile. In contrast to the BAMs, the calibration constant of the SRM changes depending on the operation mode due to a dependence of the calibration constant on the horizontal beam profile. Hence, a recalibration of the SRM is required for different operation modes. While the dynamic range of the SRM increased by a factor of 5 for SASE operation, the resolution decreased by about a factor of 4 at the same time.

The SRM, which consist basically of a multi-anode PMT, a commercial photo lens and bunch-synchronous read-out ADCs, has shown performance limitations compared to the BAMs. On the other hand, the BAMs require

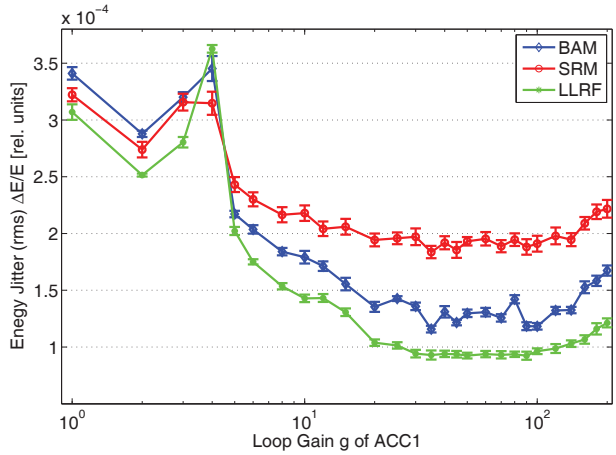

Figure 9: Relative energy jitter versus ACC1 loop gain g obtained with the BAMs, SRM and LLRF system at SASE operation.

the complex infrastructure of a laser-based synchronization system including fibre links with femtosecond timing stability.

Measurements of the beam energy jitter have been performed with the BAMs and SRM for different feedback gains g of the ACC1 LLRF controller and the results have been compared to data deduced from the in-loop RF field detection of the LLRF system. At on-crest operation, excellent agreement between the data of all 3 devices was found for feedback gains $g = 40 - 140$ with deviations of less than $1.0\ 10^{-5}$ between the devices. The optimum loop gain of the proportional controller for the lowest energy jitter of $7.6 \pm 0.3\ 10^{-5}$ (BAM measurement) was found to be at about $g \approx 80$, which is higher compared to previous studies ($g = 10 - 15$, see Fig. 4 in Ref. [5]) and in good agreement with predictions based on noise characterization of sub-components (see Fig. 4 in Ref. [6]).

REFERENCES

[1] Ch. Gerth, "Synchrotron Radiation Monitor for Energy Spectrum Measurements in the Bunch Compressors at FLASH", DIPAC'07, Venice, TUPC03.

[2] A. Wilhelm and Ch. Gerth, "Synchrotron Radiation Monitor for Bunch-Resolved Beam Energy Measurements at FLASH", DIPAC'09, Basel, TUPD43.

[3] M.K. Bock *et al.*, "New Beam Arrival Time Monitor used in a Time-Of-Flight Injector Measurement", FEL'09, Liverpool, WEPC66.

[4] S. Schulz *et al.*, "Progress Towards a Permanent Optical Synchronization Infrastructure at FLASH", FEL'09, Liverpool, WEPC72.

[5] E. Vogel *et al.*, "Beam Loading Compensation Using Real Time Bunch Charge Information from a Toroid Monitor at FLASH", PAC'07, Albuquerque, WEPMN012.

[6] F. Ludwig *et al.*, "Phase stability of the next generation RF field control for VUV- and X-Ray free electron laser", EPAC'06, Edinburgh, TUPCH188.

ISBN 978-3-95450-117-5